



# Multi-component analysis of position-velocity cubes of the HH 34 jet

B21



A. Rodríguez-González<sup>1</sup>, A. Esquivel<sup>1</sup>, A. C. Raga<sup>1</sup>, J. Cantó<sup>2</sup>, & A. Rieras

<sup>1</sup> ICN-UNAM, <sup>2</sup> IA-UNAM, <sup>3</sup> Departamento de Física e Ingeniería Nuclear, Universidad Politécnica de Cataluña

2012, Astronomy Journal, 143, 60.

We present an analysis of H spectra of the HH 34 jet with 2D spectral resolution. We carry out multi-Gaussian fits to the spatially resolved line profiles, and derive maps of the intensity, radial velocity and velocity width of each of the components. We find that close to the outflow source we have three components a high (negative) radial velocity component with a well-collimated, jet-like morphology, an intermediate velocity component with a broader morphology, and a positive radial velocity component with a non-collimated morphology and large line width.

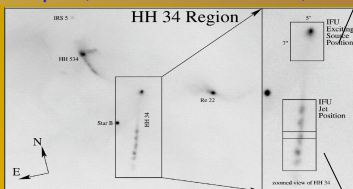
## INTRODUCTION

HH 34 is one of the best studied of all Herbig-Haro objects. It is an "aligned knot chain/large bow shock" jet was discovered by Reipurth et al. (1986). We carry out fits, of H $\alpha$  observed spectra with two or three Gaussian components, and study the spatial distribution of the resulting "high" (negative), "low" and "positive" velocity components (HVC, LVC and PVC, respectively), the PVC being present only in the region around the outflow source.

We use this analysis to present a new code for fitting multi-parametric functions to astronomical data. This code is based on the AGA (Asexual Genetic Algorithm) method developed by Canto et al. (2009) The new code(available on the web) is described below in this poster.

## OBSERVATIONS

We use were obtained in 2003 February with the Gemini Multi-Object Spectrograph Integral Field Unit (GMOS IFU) at the Gemini North Fredrick C. Gillett Telescope. (see Beck et al. 2007).

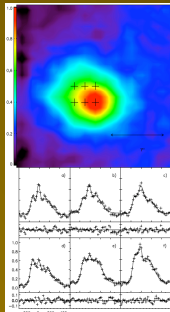


Above figure shows an H $\alpha$  image of the HH 34 jet, and zoom on the right shows the three positions for which IFU spectral imaging data were obtained :  
• exciting source : a field sampling the region of the jet close to the outflow source,  
• jet : two overlapping fields sampling the region of bright knots along the HH 34 jet, at distances of 15'' x 30'' from the outflow source.

## SPATIAL DISTRIBUTION:

### The source region:

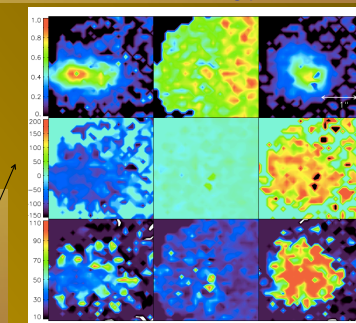
The HVC and the LVC can be interpreted as a high velocity, central component surrounded by a lower velocity, less well collimated flow. These two components are consistent a DG Tauri, who also find a narrow, jet-like feature at high velocities surrounded by broader emission at lower radial velocities. The PVC shows a centrally peaked emission distribution, centered on the point at which the jet becomes visible.



H $\alpha$  image of the "source" region, and the observed spectra and resulting 3-Gaussian + constant continuum fits at a few positions (marked with crosses) in the region with stronger emission.

Top: H $\alpha$  map of the region closer to the source. Bottom: sample of the observed spectra, their

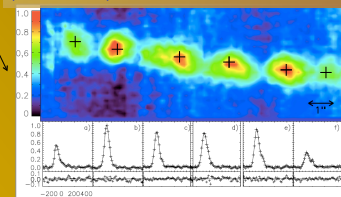
locations are marked by crosses on the map above. The solid line corresponds to the fit, and the overlying crosses denote the observational data. At the bottom of each spectra we present the residuals from the fitting procedure.



Above figure shows the results of the fit of 3 Gaussian components near the source of HH34. The left column corresponds to the high negative velocity component, the middle column to the low velocity component, and the right column to the positive velocity component.

### The jet region

The H $\alpha$  line profiles in the field along the jet only have two components (as no emission with positive radial velocities is detected) and no continuum (constant) emission.



Top: H $\alpha$  map of the jet region to the source (the direction towards the HH 34 source is to the right). Bottom: sample of the observed spectra, their locations are marked by crosses on the map above. The solid line corresponds to the fit, and the overlying crosses denote the observational data. At the bottom of each spectra we present the residuals from the fitting procedure.

## CONCLUSION

We present a new code for fitting multi-parametric functions to astronomical data. We apply this code to fitting multiple Gaussians to the H $\alpha$  position-velocity data cubes of 2 regions of HH34 (the source and the jet).

In the source region we see 3 components, the HVC, LVC and PVC. PVC would be expected for H $\alpha$  jet emission which is being scattered in an approximately stationary, dusty circumstellar envelope.

In the "jet" region we see two components: a HVC with a somewhat narrower intensity distribution than a LVC.

## AGA-v1

<http://www.nucleares.unam.mx/astroplasmas/>

The basic idea of genetic algorithms is to optimize a function  $f$  in an  $n$ -dimensional space, that is  $f(q) = f(q_1, q_2, q_3, \dots, q_n)$ . The coordinates of a single point in the  $n$ -dimensional space (a set of  $q$ ) constitutes what we will call an individual. To find the set of  $q$  values that optimize  $f$ :

1. Produce a  $N_{par}$  parents, each parent reproduces asexually, to produce  $N_k = (N_{ind}/N_{parents}) - 1$  sons.
2. The level of fitness of each individual is computed and stored. The fitness level corresponds to the value of a merit function, typically a  $\chi^2$  constructed from a target function  $g$ .
3. The entire population is ranked and ordered based on the fitness level. The first  $N_{parents}$  individuals in the list (the fittest, e.g. those with the minimum  $\chi^2$ ) are selected to continue to the next generation (they become parents), the rest of the individuals are discarded.
4. The criteria for stopping the algorithm are evaluated. If the criteria are fulfilled, the program returns the best solution (fittest individual) and an estimate of the uncertainties. If the criteria are not met, the programs continues to step (1).
5. The size of the hyper-boxes (which determines the region of parameter space to be sampled) is adjusted.

Beck et al. 2007, AJ, 133, 1221.  
Canto et al. 2009, ApJ, 501, 1259.  
Reipurth et al. 1986, A&A, 164, 51.

Other application see poster

A30